基于介电弹性体驱动器的软体机器人建模与跟踪控制

王亚午[1,2,3], 叶雯珺[3], 张一龙[3,4], 赖旭芝[1,2], 吴 敏[1,2], 苏春翌[3†]

(1. 中国地质大学(武汉) 自动化学院, 湖北 武汉 430074;
2. 复杂系统先进控制与智能自动化湖北省重点实验室, 湖北 武汉 430074;
3. 康考迪亚大学 工程与计算机科学学院, 蒙特利尔 魁北克 H3G 1M8;
4. 东北电力大学 自动化工程学院, 吉林 吉林 132012)

摘要: 针对基于介电弹性体驱动器的软体机器人的跟踪控制问题, 本文提出一种自适应鲁棒控制策略. 根据虚功原理建立介电弹性体驱动器的动力学模型, 模型中弹性势能部分采用Gent模型进行描述. 考虑到介电弹性体驱动器的精确模型参数难以获取, 使用基于径向基神经网络的逼近器对模型中的未知项进行估计. 同时, 考虑到介电弹性体驱动器形变量的变化率难以被测量, 设计状态观测器对系统未知状态量进行观测. 根据逼近器的估计结果和状态观测器的观测结果, 设计滑模控制器实现介电弹性体驱动器的跟踪控制目标. 最后, 通过数值仿真实验验证所提控制策略的有效性.

关键词: 介电弹性体驱动器; Gent模型; 径向基网络; 状态观测器; 滑模控制

引用格式: 王亚午, 叶雯珺, 张一龙, 等. 基于介电弹性体驱动器的软体机器人建模与跟踪控制. 控制理论与应用, 2020, 37(4): 871 – 880

DOI:10.7641/CTA.2019.80965

Modeling and tracking control for soft robots of dielectric elastomer actuators

WANG Ya-wu[1,2,3], YE Wen-jun[3], ZHANG Yi-long[3,4], LAI Xu-zhi[1,2],
WU Min[1,2], SU Chun-Yi[3†]

(1. School of Automation, China University of Geosciences (Wuhan), Wuhan Hubei 430074, China;
2. Hubei Key Laboratory of Advanced Control and Intelligent Automation for Complex Systems, Wuhan Hubei 430074, China;
3. Faculty of Engineering and Computer Science, Concordia University, Montreal Quebec H3G 1M8, Canada;
4. School of Automation Engineering, Northeast Electric Power University, Jilin Jilin 132012, China)

Abstract: This paper proposes an adaptive robust control strategy for dielectric elastomer actuators (DEAs) utilized in soft robots to achieve their tracking control. The dynamic model of the DEA is developed based on the principle of virtual work, whose elastic energy is described by the Gent model. Since the model parameters of the DEA are difficult to obtain, two approximators based on the radial basis function neural networks (RBFNNs) are employed to estimate the unknown items of the dynamic model. Meanwhile, due to the fact that the rate of the stretch of the DEA is difficult to measure, the state observer is designed to estimate the system states. Based on the approximation results and the observed states, the sliding mode controller (SMC) is designed to realize the trajectory tracking control of the DEA. Finally, the simulation results demonstrate the effectiveness of the proposed control strategy.

Key words: dielectric elastomer actuator; Gent model; radial basis function networks; state observer; sliding mode control

Citation: WANG Yawu, YE Wenjun, ZHANG Yilong, et al. Modeling and tracking control for soft robots of dielectric elastomer actuators. *Control Theory & Applications*, 2020, 37(4): 871 – 880

1 Introduction

Due to the capability of large deformation and shape changes, the dielectric elastomer actuator (DEA) shows promising applications in the field of soft robotics[1]. The DEA consists of a soft membrane sandwiched between two compliant electrodes on two surfaces[2]. When a voltage is applied to the electrodes, the dielectric elastomer membrane reduces in thickness and expands in area[3]. Because the DEA has the advantages of high-strain response, high energy density and fast response time[4], the soft robots driven by the DEA are widely used in various application-

Received 10 December 2018; accepted 10 September 2019.
†Corresponding author. E-mail: cysu@alcor.concordia.ca.
Recommended by Associate Editor: WU Yu-qiang.
Supported by the National Natural Science Foundation for Young Scientists of China (61903344) and the National Natural Science Foundation of China (61733006).

s, such as artificial muscles[5], bionic robots[6], microelectromechanical systems (MEMS)[7] and so on.

The mathematical modeling of the DEA is the basis for understanding its characteristics, and is also the premise to design the model based controller. In general, the mathematical modeling methods of the DEA are divided into two categories: the physical-based modeling approach and the phenomenological modeling approach. The physical-based modelling approach is mainly based on the physical principles. The mathematical model is obtained by analyzing the energy conversion mechanism during the deformation process of the DEA. This modeling technique has the advantages of explicitness and preciseness. Based on the continuum mechanics theory and the thermodynamic theory, [8] explains the physical-based modeling approach of the DEA in detail. On the other hand, unlike the physical-based approach, the phenomenological modeling approach is mainly based on the experimental phenomenons. By analyzing the experimental data, one can use the combination of physical components (such as, resistor, capacitor, spring and dashpot) to represent the model of the DEA. This technique has the advantages of simplicity and efficiency. [9] employs capacitors and resistors to describe the electrical model of the DEA, and employs springs and dashpots to describe the mechanical model of the DEA. These two models can be connected through the Maxwell force, together to provide a mathematical model of the DEA.

Currently, the complete understanding of the nonlinear dynamic behaviors of the DEA with a general model is still an open challenge. Researches on the DEA mainly focus on materials and physics, while few efforts are made from the control point of view. However, [10] proposes a feedforward control strategy for the DEA. [11] designs the PID controller for the DEA. In general, the model of the DEA usually contains unmeasurable parameters (or parameter perturbations) and external disturbances, so it is meaningful to invistigate the adaptive robust control of the DEA. Meantime, in actual control, some states of the DEA are difficult to obtain, so an effective state observer is required for the actual control of the DEA. In this respect, it is an urgent demand to develop an implementable controller for the DEA, which can take the dynamic of the DEA into the consideration, tolerate the parameter uncertainties, and also work with limited measurable states.

In this paper, we propose an adaptive robust control strategy for the DEA to realize its trajectory tracking control objective. According to the principle of virtual work, the elastic energy of the DEA is described by the Gent model, and then the dynamic model of the DEA is developed. Since the model parameters of the DEA are difficult to obtain, we use two approximators based on the radial basis function neural networks (RBFNNs) to estimate the unknown items of the model. Meantime, since the rate of the stretch of the DEA is difficult to measure, we design a state observer to estimate the system states only according to the measured value of the stretch. According to the approximation results and the observed states, we design the sliding mode controller (SMC) to realize the trajectory tracking control of the DEA. Finally, the simulation results demonstrate the effectiveness of the proposed control strategy.

2 Dynamic model

In this section, the dynamic model of the DEA is developed based on the principle of virtual work.

Figure 1 shows the actuation mechanism of the DEA[12], where Fig. 1(a) shows the un-deformed state of the DEA and Fig. 1(b) shows the deformed state of the DEA. In the Fig. 1, L_1, L_2 and L_3 are dimensions corresponding to the un-deformed state; l_1, l_2 and l_3 are dimensions corresponding to the deformed state; P_1 and P_2 are tensile forces; Φ is the voltage; $\bar{Q}$ is the charge.

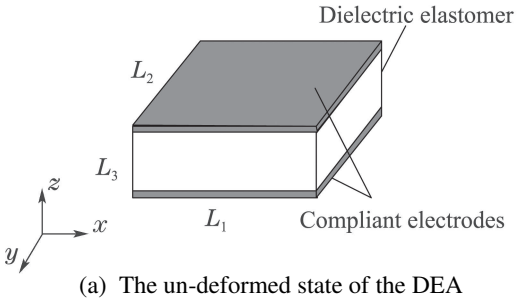

(a) The un-deformed state of the DEA

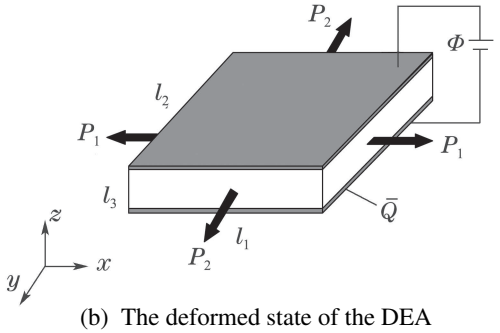

(b) The deformed state of the DEA

Fig. 1 Model of DEA

We define $\lambda_1 = l_1/L_1,\ \lambda_2 = l_2/L_2$ and $\lambda_3 = l_3/L_3$. Since the DEA is incompressible,

$$\lambda_1\lambda_2\lambda_3 = 1. \tag{1}$$

The relationship between the charge $\bar{Q}$ and the voltage Φ is[8]

$$\bar{Q} = \Phi\frac{\varepsilon(\lambda_1, \lambda_2, T)}{L_3/(L_1L_2)}\lambda_1^2\lambda_2^2, \tag{2}$$

where T is the environment temperature; $\varepsilon(\lambda_1, \lambda_2, T)$ is the permittivity of the DEA, which is a nonlinear function of $\lambda_1,\ \lambda_2$ and T.

When there are minor changes of dimensions of the DEA ($\delta\lambda_1$ and $\delta\lambda_2$), the works done by the tensile forces are $P_1L_1\delta\lambda_1$ and $P_2L_2\delta\lambda_2$, and the work done

by the voltage is $\Phi\delta\bar{Q}$. Thus, the variation of the charge is

$$\begin{aligned}&\delta\bar{Q}=\\&\frac{\varepsilon(\lambda_1,\lambda_2,T)}{L_3/(L_1L_2)}\lambda_1^2\lambda_2^2\delta\Phi+2\Phi\frac{\varepsilon(\lambda_1,\lambda_2,T)}{L_3/(L_1L_2)}\lambda_1\lambda_2^2\delta\lambda_1+\\&\Phi\frac{1}{L_3/(L_1L_2)}\lambda_1^2\lambda_2^2\frac{\partial\varepsilon(\lambda_1,\lambda_2,T)}{\partial\lambda_1}\delta\lambda_1+\\&\Phi\frac{1}{L_3/(L_1L_2)}\lambda_1^2\lambda_2^2\frac{\partial\varepsilon(\lambda_1,\lambda_2,T)}{\partial\lambda_2}\delta\lambda_2+\\&2\Phi\frac{\varepsilon(\lambda_1,\lambda_2,T)}{L_3/(L_1L_2)}\lambda_2\lambda_1^2\delta\lambda_2.\end{aligned}\tag{3}$$

The inertia forces in each material element along the x-direction and y-direction are $\rho L_2L_3x^2(\frac{\mathrm{d}^2\lambda_1}{\mathrm{d}t^2})$ and $\rho L_1L_3y^2(\frac{\mathrm{d}^2\lambda_2}{\mathrm{d}t^2})$, respectively[13]. ρ is the density of the DEA. The damping forces in each material element along the x-direction and y-direction are $cx(\frac{\mathrm{d}\lambda_1}{\mathrm{d}t})$ and $cy(\frac{\mathrm{d}\lambda_2}{\mathrm{d}t})$, respectively. c is the damping coefficient of the DEA[14]. Thus, the works done by the inertial force and the damping force are

$$\begin{cases}\rho L_2L_3\dfrac{\mathrm{d}^2\lambda_1}{\mathrm{d}t^2}\delta\lambda_1\displaystyle\int_0^{L_1}x^2\mathrm{d}x=\frac{L_1^3\rho L_2L_3}{3}\frac{\mathrm{d}^2\lambda_1}{\mathrm{d}t^2}\delta\lambda_1,\\ \rho L_1L_3\dfrac{\mathrm{d}^2\lambda_2}{\mathrm{d}t^2}\delta\lambda_2\displaystyle\int_0^{L_2}y^2\mathrm{d}y=\frac{L_2^3\rho L_1L_3}{3}\frac{\mathrm{d}^2\lambda_2}{\mathrm{d}t^2}\delta\lambda_2,\\ c\dfrac{\mathrm{d}\lambda_1}{\mathrm{d}t}\delta\lambda_1\displaystyle\int_0^{L_1}x\mathrm{d}x=\frac{cL_1^2\delta\lambda_1}{2}\frac{\mathrm{d}\lambda_1}{\mathrm{d}t},\\ c\dfrac{\mathrm{d}\lambda_2}{\mathrm{d}t}\delta\lambda_2\displaystyle\int_0^{L_2}y\mathrm{d}y=\frac{cL_2^2\delta\lambda_2}{2}\frac{\mathrm{d}\lambda_2}{\mathrm{d}t}.\end{cases}\tag{4}$$

According to the thermodynamics theory and the principle of virtual work, the variation of the free energy (W) of the DEA is equal to the works done by the voltage, the tensile forces, the inertia forces, and the damping forces. So,

$$\begin{aligned}L_1L_2L_3\delta W=&\Phi\delta\bar{Q}+P_1L_1\delta\lambda_1+P_2L_2\delta\lambda_2-\\&\frac{L_1^3\rho L_2L_3}{3}\frac{\mathrm{d}^2\lambda_1}{\mathrm{d}t^2}\delta\lambda_1-\frac{cL_1^2\delta\lambda_1}{2}\frac{\mathrm{d}\lambda_1}{\mathrm{d}t}-\\&\frac{L_2^3\rho L_1L_3}{3}\frac{\mathrm{d}^2\lambda_2}{\mathrm{d}t^2}\delta\lambda_2-\frac{cL_2^2\delta\lambda_2}{2}\frac{\mathrm{d}\lambda_2}{\mathrm{d}t}.\end{aligned}\tag{5}$$

Moreover, W is consisted of the elastic energy (W_{ela}) and the electric energy (W_{ele})[13], that is

$$\begin{aligned}&W=W_{\mathrm{ela}}+W_{\mathrm{ele}}=\\&-\frac{\mu(T)J_{\mathrm{m}}}{2}\ln(1-\frac{\lambda_1^2+\lambda_2^2+\lambda_1^{-2}\lambda_2^{-2}-3}{J_{\mathrm{m}}})+\\&\frac{\varepsilon(\lambda_1,\lambda_2,T)}{2}(\frac{\Phi}{L_3})^2\lambda_1^2\lambda_2^2,\end{aligned}\tag{6}$$

where $\mu(T)$ is the shear modulus of the DEA, which depends on the environment temperature T; J_{m} is the deformation limit.

Remark 1 According to the superelastic material theory, the Gent model is chosen to describe the elastic energy in this paper[15]. However, one can choose the other model, such as, Neo-Hookean model, Mooney-Rivlin model, Ogden model, Arruda-Boyce model, and so on.

Submitting (3) into (5), we obtain

$$\begin{aligned}&L_1L_2L_3\delta W=\\&\Phi\frac{\varepsilon(\lambda_1,\lambda_2,T)}{L_3/(L_1L_2)}\lambda_1^2\lambda_2^2\delta\Phi+P_1L_1\delta\lambda_1+\\&2\Phi^2\frac{\varepsilon(\lambda_1,\lambda_2,T)}{L_3/(L_1L_2)}\lambda_1\lambda_2^2\delta\lambda_1+P_2L_2\delta\lambda_2+\\&\Phi^2\frac{\varepsilon(\lambda_1,\lambda_2,T)}{L_3/(L_1L_2)}\lambda_1^2\lambda_2^2\frac{\partial\varepsilon(\lambda_1,\lambda_2,T)}{\partial\lambda_1}\delta\lambda_1+\\&\Phi^2\frac{\varepsilon(\lambda_1,\lambda_2,T)}{L_3/(L_1L_2)}\lambda_1^2\lambda_2^2\frac{\partial\varepsilon(\lambda_1,\lambda_2,T)}{\partial\lambda_2}\delta\lambda_2+\\&2\Phi^2\frac{\varepsilon(\lambda_1,\lambda_2,T)}{L_3/(L_1L_2)}\lambda_2\lambda_1^2\delta\lambda_2-\\&\frac{L_1^3\rho L_2L_3}{3}\frac{\mathrm{d}^2\lambda_1}{\mathrm{d}t^2}\delta\lambda_1-\frac{cL_1^2\delta\lambda_1}{2}\frac{\mathrm{d}\lambda_1}{\mathrm{d}t}-\\&\frac{L_2^3\rho L_1L_3}{3}\frac{\mathrm{d}^2\lambda_2}{\mathrm{d}t^2}\delta\lambda_2-\frac{cL_2^2\delta\lambda_2}{2}\frac{\mathrm{d}\lambda_2}{\mathrm{d}t}.\end{aligned}\tag{7}$$

By solving (7), the partial differentials of the free energy are given by

$$\begin{cases}\dfrac{\partial W}{\partial\lambda_1}=2\varepsilon(\lambda_1,\lambda_2,T)(\dfrac{\Phi}{L_3})^2\lambda_1\lambda_2^2+\dfrac{P_1}{L_2L_3}-\\ \qquad\dfrac{L_1^2\rho}{3}\dfrac{\mathrm{d}^2\lambda_1}{\mathrm{d}t^2}-\dfrac{1}{2}\dfrac{cL_1}{L_2L_3}\dfrac{\mathrm{d}\lambda_1}{\mathrm{d}t}+\\ \qquad(\dfrac{\Phi}{L_3})^2\dfrac{\partial\varepsilon(\lambda_1,\lambda_2,T)}{\partial\lambda_1}\lambda_1^2\lambda_2^2,\\ \dfrac{\partial W}{\partial\lambda_2}=2\varepsilon(\lambda_1,\lambda_2,T)(\dfrac{\Phi}{L_3})^2\lambda_2\lambda_1^2+\dfrac{P_2}{L_1L_3}-\\ \qquad\dfrac{L_2^2\rho}{3}\dfrac{\mathrm{d}^2\lambda_2}{\mathrm{d}t^2}-\dfrac{1}{2}\dfrac{cL_2}{L_1L_3}\dfrac{\mathrm{d}\lambda_2}{\mathrm{d}t}+\\ \qquad(\dfrac{\Phi}{L_3})^2\dfrac{\partial\varepsilon(\lambda_1,\lambda_2,T)}{\partial\lambda_2}\lambda_1^2\lambda_2^2.\end{cases}\tag{8}$$

Submitting (6) into (8), the dynamic model of the DE is derived as

$$\begin{aligned}\frac{L_1^2\rho}{3\mu(T)}\frac{\mathrm{d}^2\lambda_1}{\mathrm{d}t^2}=&-\frac{\lambda_1-\lambda_1^{-3}\lambda_2^{-2}}{1-\dfrac{\lambda_1^2+\lambda_2^2+\lambda_1^{-2}\lambda_2^{-2}-3}{J_{\mathrm{m}}}}+\\&(\frac{\Phi}{L_3})^2\frac{\varepsilon(\lambda_1,\lambda_2,T)}{\mu(T)}\lambda_1\lambda_2^2+\\&(\frac{\Phi}{L_3})^2\frac{\partial\varepsilon(\lambda_1,\lambda_2,T)}{2\partial\lambda_1}\frac{\lambda_1^2\lambda_2^2}{\mu(T)}-\\&\frac{1}{2}\frac{cL_1}{\mu(T)L_2L_3}\frac{\mathrm{d}\lambda_1}{\mathrm{d}t}+\frac{P_1}{\mu(T)L_2L_3},\end{aligned}$$

$$\frac{L_2^2\rho}{3\mu(T)}\frac{\mathrm{d}^2\lambda_2}{\mathrm{d}t^2}=-\frac{\lambda_2-\lambda_2^{-3}\lambda_1^{-2}}{1-\dfrac{\lambda_1^2+\lambda_2^2+\lambda_1^{-2}\lambda_2^{-2}-3}{J_{\mathrm{m}}}}+(\frac{\Phi}{L_3})^2\frac{\varepsilon(\lambda_1,\lambda_2,T)}{\mu(T)}\lambda_2\lambda_1^2+(\frac{\Phi}{L_3})^2\frac{\partial\varepsilon(\lambda_1,\lambda_2,T)}{2\partial\lambda_2}\frac{\lambda_1^2\lambda_2^2}{\mu(T)}-\frac{1}{2}\frac{cL_2}{\mu(T)L_1L_3}\frac{\mathrm{d}\lambda_2}{\mathrm{d}t}+\frac{P_2}{\mu(T)L_1L_3}. \tag{9}$$

We assume that $L_1=L_2=L$ and $P_1=P_2=P$. Meantime, we also assume that the DEA is isotropic. So, $\lambda_1=\lambda_2=\lambda$, and (9) is reduced to

$$\frac{L^2\rho}{3\mu(T)}\ddot{\lambda}+\frac{1}{2}\frac{c}{\mu(T)L_3}\dot{\lambda}=(\frac{\Phi}{L_3})^2\frac{\varepsilon(\lambda,T)}{\mu(T)}\lambda^3+\frac{P}{\mu(T)LL_3}+(\frac{\Phi}{L_3})^2\frac{\partial\varepsilon(\lambda,T)}{2\partial\lambda}\frac{\lambda^4}{\mu(T)}-\frac{\lambda-\lambda^{-5}}{1-\dfrac{2\lambda^2+\lambda^{-4}-3}{J_{\mathrm{m}}}}. \tag{10}$$

Let $x=[X_1\ \ X_2]^{\mathrm{T}}=[\lambda\ \ \dot{\lambda}]^{\mathrm{T}}$, then the state-space model of the DEA is

$$\begin{cases}\dot{X}_1=X_2,\\ \dot{X}_2=f(x)+g(x)u+d_t,\end{cases} \tag{11}$$

where

$$f(x)=\frac{\dfrac{P}{\mu(T)LL_3}-\dfrac{1}{2}\dfrac{cX_2}{\mu(T)L_3}-\dfrac{X_1-X_1^{-5}}{1-\dfrac{2X_1^2+X_1^{-4}-3}{J_{\mathrm{m}}}}}{\dfrac{L^2\rho}{3\mu(T)}}, \tag{12}$$

$$g(x)=\frac{\dfrac{\varepsilon(X_1,T)}{\mu(T)}X_1^3+\dfrac{\partial\varepsilon(X_1,T)}{2\partial\lambda}\dfrac{X_1^4}{\mu(T)}}{\dfrac{L_3^2L^2\rho}{3\mu(T)}}, \tag{13}$$

$$u=\Phi^2, \tag{14}$$

and d_t is the external disturbance, $|d_t|\leqslant d_{\mathrm{d}}$.

3 Approximators and observer design

When (11) is obtained, we can design the controller that is based on the model parameters and all system states to realize the control of the DEA. However, in actual control, the model parameters of the DEA (i.e. ρ, $\mu(T)$, c, $\varepsilon(\lambda,T)$, $\dfrac{\partial\varepsilon(\lambda,T)}{\partial\lambda}$ and J_{m}) are unknown. Although λ can be measured by using the laser displacement sensor, $\dot{\lambda}$ is not measurable. As a result, $f(x)$, $g(x)$ and $\dot{\lambda}$ are unknown.

In order to meet the demand of the actual control, the approximators should be constructed to estimate $f(x)$ and $g(x)$, and the state observer should be designed to acquire $\dot{\lambda}$. Considering that the RBFNN can approximate any nonlinear function with any precision[16], and it has the advantages of fast convergence speed and avoiding the local minimum problem, we prefer to choose the RBFNN to construct the approximator. Since both $f(x)$ and $g(x)$ are unknown, a simple way is to design two RBFNN-based approximators to approximate $f(x)$ and $g(x)$, respectively. Moreover, when the number of the hidden layer nodes is sufficient, the approximation error of the three-layer RBFNN (input-layer, hidden-layer and output layer) for any nonlinear function is small enough[17]. So, we use the RBFNN with such simple topologies for convenience.

It is noted that there exist other effective parameter estimation methods (such as [18–20] and so on), which can be employed to construct the approximator. However, the purpose of this paper is to present a feasible tracking control strategy for the DEA utilized in soft robots. So, next we will only show the construct procedure of the RBFNN-based approximator in detail. Interested readers may solve such open problem by employing other parameter estimation methods.

(11) can be rewritten as

$$\begin{cases}\dot{x}=Ax+b[f(x)+g(x)u+d_t],\\ y=C^{\mathrm{T}}x,\end{cases} \tag{15}$$

where $A=[0\quad 1;0\quad 0]$, $b=[0\ \ 1]^{\mathrm{T}}$ and $C=[1\ \ 0]^{\mathrm{T}}$; y is the output of the system.

The state observer is designed to be

$$\begin{cases}\dot{\hat{x}}=A\hat{x}+b[\hat{f}(\hat{x})+\hat{g}(\hat{x})u-v]+K(y-C^{\mathrm{T}}\hat{x}),\\ \hat{y}=C^{\mathrm{T}}\hat{x},\end{cases} \tag{16}$$

where $\hat{x}$ is the observed value of x; $\hat{f}(\hat{x})$ and $\hat{g}(\hat{x})$ are the estimated values of $f(x)$ and $g(x)$, respectively; $K=[k_1\ \ k_2]^{\mathrm{T}}$; v is the robustifying item;

$$\begin{cases}\hat{f}(\hat{x})=\hat{W}_1^{\mathrm{T}}\hat{\sigma}_1,\\ \hat{g}(\hat{x})=\hat{W}_2^{\mathrm{T}}\hat{\sigma}_2,\end{cases} \tag{17}$$

$$\begin{cases}\hat{\sigma}_1=[\hat{\sigma}_{11}\ \ \hat{\sigma}_{12}\ \ \cdots\ \ \hat{\sigma}_{1N_1}]^{\mathrm{T}},\\ \hat{\sigma}_2=[\hat{\sigma}_{21}\ \ \hat{\sigma}_{22}\ \ \cdots\ \ \hat{\sigma}_{2N_2}]^{\mathrm{T}},\\ \hat{W}_1=[\hat{W}_{11}\ \ \hat{W}_{12}\ \ \cdots\ \ \hat{W}_{1N_1}]^{\mathrm{T}},\\ \hat{W}_2=[\hat{W}_{21}\ \ \hat{W}_{22}\ \ \cdots\ \ \hat{W}_{2N_2}]^{\mathrm{T}},\end{cases} \tag{18}$$

$$\hat{\sigma}_{ij}=\exp(\frac{\|\hat{x}-\chi_{ij}\|^2}{2\psi_i})(i=1,2\text{ and }j=1,2,\cdots,N_i), \tag{19}$$

$\hat{W}_1$ and $\hat{W}_2$ are the actual weight vectors of two RBFNNs, respectively; $\hat{\sigma}_1$ and $\hat{\sigma}_2$ are the actual output vectors of Gauss functions of two RBFNNs, respective-

ly; N_1 and N_2 are the node numbers of the hidden layer of two RBFNNs, respectively; χ_{ij}=$[\chi'_{ij}\ \ \chi''_{ij}]^{\mathrm{T}}$ are constant vectors; ψ_i are constants.

Moreover, it is known that

$$\begin{cases} f(x) = W_1^{\mathrm{T}}\sigma_1 + \varepsilon_1^*, \\ g(x) = W_2^{\mathrm{T}}\sigma_2 + \varepsilon_2^*, \end{cases} \tag{20}$$

where W_1 and W_2 are the ideal weight vectors of two RBFNNs, respectively; σ_1 and σ_2 are the ideal output vectors of Gauss functions of two RBFNNs, respectively; ε_1^* and ε_2^* are approximation errors of two RBFNNs, respectively; W_1, W_2, ε_1^* and ε_2^* are bounded, that is

$$\begin{cases} \|W_1\| \leqslant W_{1\mathrm{M}},\ \|W_2\| \leqslant W_{2\mathrm{M}}, \\ \varepsilon_1^* \leqslant \varepsilon_{1\mathrm{M}}^*,\ \varepsilon_2^* \leqslant \varepsilon_{2\mathrm{M}}^*, \\ W_{1\mathrm{M}} > 0,\ W_{2\mathrm{M}} > 0, \\ \varepsilon_{1\mathrm{M}}^* > 0,\ \varepsilon_{2\mathrm{M}}^* > 0. \end{cases} \tag{21}$$

Using (15) minus (16) yields

$$\begin{cases} \dot{\tilde{x}} = (A - KC^{\mathrm{T}})\tilde{x} + b[\tilde{W}_1^{\mathrm{T}}\hat{\sigma}_1 + \omega_1 + \\ \qquad \varepsilon_1^* + v_1 + (\tilde{W}_2^{\mathrm{T}}\hat{\sigma}_2 + \\ \qquad \omega_2 + \varepsilon_2^*)u + d_t + v_2], \\ \tilde{y} = C^{\mathrm{T}}\tilde{x}, \end{cases} \tag{22}$$

where $\tilde{x} = x - \hat{x}$; $\tilde{W}_1 = W_1 - \hat{W}_1$, $\tilde{W}_2 = W_2 - \hat{W}_2$; $v = v_1 + v_2$; $\omega_1 = W_1^{\mathrm{T}}[\sigma_1 - \hat{\sigma}_1]$, $\omega_2 = W_2^{\mathrm{T}}[\sigma_2 - \hat{\sigma}_2]$; ω_1 and ω_2 are bounded, that is

$$\begin{cases} \|\omega_1\| \leqslant \beta_1,\ \beta_1 > 0, \\ \|\omega_2\| \leqslant \beta_2,\ \beta_2 > 0. \end{cases} \tag{23}$$

According to (22),

$$\tilde{y} = H(s)L(s)\Delta, \tag{24}$$

where $H(s) = C^{\mathrm{T}}(sI - A)^{-1}b$; s denotes the differential operator $\dfrac{\mathrm{d}}{\mathrm{d}t}$; $L^{-1}(s)$ is a transfer function with stable poles and $L(s)$ is chosen to ensure that $H(s)L(s)$ is strictly positive realness (SPR);

$$\begin{cases} \Delta = \delta_1 + \delta_2 + \tilde{W}_1^{\mathrm{T}}\hat{\bar{\sigma}}_1 + \tilde{W}_2^{\mathrm{T}}\hat{\bar{\sigma}}_2 u + \\ \qquad (\bar{\omega}_2 + \bar{\varepsilon}_2)u + \bar{\omega}_1 + \bar{\varepsilon}_1 + \bar{d}_t + \bar{v}_1 + \bar{v}_2, \\ \delta_1 = L^{-1}(s)[\tilde{W}_1^{\mathrm{T}}\hat{\sigma}_1] - \tilde{W}_1^{\mathrm{T}}L^{-1}(s)[\hat{\sigma}_1], \\ \delta_2 = L^{-1}(s)[\tilde{W}_2^{\mathrm{T}}\hat{\sigma}_2 u] - \tilde{W}_2^{\mathrm{T}}L^{-1}(s)[\hat{\sigma}_2]u, \\ \hat{\bar{\sigma}}_1 = L^{-1}(s)[\hat{\sigma}_1],\ \hat{\bar{\sigma}}_2 = L^{-1}(s)[\hat{\sigma}_2], \\ \bar{\omega}_1 = L^{-1}(s)\omega_1,\ \bar{\omega}_2 = L^{-1}(s)\omega_2, \\ \bar{\varepsilon}_1 = L^{-1}(s)\varepsilon_1^*,\ \bar{\varepsilon}_2 = L^{-1}(s)\varepsilon_2^*, \\ \bar{v}_1 = L^{-1}(s)[v_1],\ \bar{v}_2 = L^{-1}(s)[v_2], \\ \bar{d}_t = L^{-1}(s)[\bar{d}_t], \end{cases} \tag{25}$$

δ_1 and δ_2 are bounded, that is

$$\begin{cases} \|\delta_1\| \leqslant c_1\|\tilde{W}_1\|_{\mathrm{F}},\ c_1 > 0, \\ \|\delta_2\| \leqslant c_2\|\tilde{W}_2\|_{\mathrm{F}},\ c_2 > 0, \end{cases} \tag{26}$$

and $\|\Theta_1\|_{\mathrm{F}}$ is Frobenius norm of Θ_1.

Letting $H(s)L(s) = C_{\mathrm{c}}^{\mathrm{T}}(sI - A_{\mathrm{c}})^{-1}b_{\mathrm{c}}$ and $\tilde{y} = C_{\mathrm{c}}^{\mathrm{T}}\tilde{z}$, then (24) can be rewritten as

$$\begin{cases} \dot{\tilde{z}} = A_{\mathrm{c}}\tilde{z} + b_{\mathrm{c}}\Delta, \\ \tilde{y} = C_{\mathrm{c}}^{\mathrm{T}}\tilde{z}. \end{cases} \tag{27}$$

Since $H(s)L(s)$ is SPR, there exists $P = P^{\mathrm{T}} > 0$, which makes

$$A_{\mathrm{c}}^{\mathrm{T}}P + PA_{\mathrm{c}} = -Q, \tag{28}$$

where $Q = Q^{\mathrm{T}} > 0$.

The Lyapunov function is constructed as

$$V = \frac{1}{2}\tilde{z}^{\mathrm{T}}P\tilde{z} + \frac{1}{2}\mathrm{tr}(\tilde{W}_1^{\mathrm{T}}F_1^{-1}\tilde{W}_1) + \frac{1}{2}\mathrm{tr}(\tilde{W}_2^{\mathrm{T}}F_2^{-1}\tilde{W}_2), \tag{29}$$

where $F_1 = F_1^{\mathrm{T}} > 0$, $F_2 = F_2^{\mathrm{T}} > 0$; $\mathrm{tr}(\Theta_2)$ is the trace of Θ_2.

The derivative of V is

$$\begin{aligned} \dot{V} = {} & \frac{1}{2}\dot{\tilde{z}}^{\mathrm{T}}P\tilde{z} + \frac{1}{2}\tilde{z}^{\mathrm{T}}P\dot{\tilde{z}} + \mathrm{tr}(\tilde{W}_1^{\mathrm{T}}F_1^{-1}\dot{\tilde{W}}_1) + \\ & \mathrm{tr}(\tilde{W}_2^{\mathrm{T}}F_2^{-1}\dot{\tilde{W}}_2) = \\ & \frac{1}{2}[A_{\mathrm{c}}\tilde{z} + b_{\mathrm{c}}\Delta]^{\mathrm{T}}P\tilde{z} + \frac{1}{2}\tilde{z}^{\mathrm{T}}P[A_{\mathrm{c}}\tilde{z} + b_{\mathrm{c}}\Delta] + \\ & \mathrm{tr}(\tilde{W}_1^{\mathrm{T}}F_1^{-1}\dot{\tilde{W}}_1) + \mathrm{tr}(\tilde{W}_2^{\mathrm{T}}F_2^{-1}\dot{\tilde{W}}_2) = \\ & \frac{1}{2}\tilde{z}^{\mathrm{T}}(A_{\mathrm{c}}^{\mathrm{T}}P + PA_{\mathrm{c}})\tilde{z} + \tilde{z}^{\mathrm{T}}Pb_{\mathrm{c}}\Delta + \\ & \mathrm{tr}(\tilde{W}_1^{\mathrm{T}}F_1^{-1}\dot{\tilde{W}}_1) + \mathrm{tr}(\tilde{W}_2^{\mathrm{T}}F_2^{-1}\dot{\tilde{W}}_2) = \\ & -\frac{1}{2}\tilde{z}^{\mathrm{T}}Q\tilde{z} + \tilde{y}\Delta + \mathrm{tr}(\tilde{W}_1^{\mathrm{T}}F_1^{-1}\dot{\tilde{W}}_1) + \\ & \mathrm{tr}(\tilde{W}_2^{\mathrm{T}}F_2^{-1}\dot{\tilde{W}}_2). \end{aligned} \tag{30}$$

To ensure the convergences of the state observer and the approximators, by employing the trial and error method, we design the update laws to be

$$\begin{cases} \dot{\hat{W}}_1 = F_1\hat{\bar{\sigma}}_1\tilde{y} - \kappa_1 F_1|\tilde{y}|\hat{W}_1, \\ \dot{\hat{W}}_2 = F_2\hat{\bar{\sigma}}_2\tilde{y}u - \kappa_2 F_2|\tilde{y}|\hat{W}_2, \end{cases} \tag{31}$$

where $\kappa_1 > 0,\ \kappa_2 > 0$.

Submitting (31) into (30) yields

$$\begin{aligned} \dot{V} = {} & \mathrm{tr}(\tilde{W}_1^{\mathrm{T}}(-\hat{\bar{\sigma}}_1\tilde{y} + \kappa_1|\tilde{y}|\hat{W}_1)) + \\ & \mathrm{tr}(\tilde{W}_2^{\mathrm{T}}(-\hat{\bar{\sigma}}_2\tilde{y}u + \kappa_2|\tilde{y}|\hat{W}_2)) - \\ & \frac{1}{2}\tilde{z}^{\mathrm{T}}Q\tilde{z} + \tilde{y}\Delta. \end{aligned} \tag{32}$$

The robustifying item in (16) is designed to be

$$v = v_1 + v_2 = -(D_1 + D_2)\mathrm{sgn}\,\tilde{y}, \tag{33}$$

where $D_1 \geqslant \beta_1\sigma_{\mathrm{M}}$, $D_2 \geqslant \beta_2\sigma_{\mathrm{M}}u_{\mathrm{d}}$, $\sigma_{\mathrm{M}} = \sigma_{\max}[L^{-1}(s)]$, $\sigma_{\max}[\Theta_3]$ is the maximum singular value of Θ_3; $|u| \leqslant u_{\mathrm{d}}$; $\mathrm{sgn}(\cdot)$ is the symbol function.

According to (23) and (33), we obtain

$$\begin{cases} \tilde{y}(\bar{\omega}_1+\bar{v}_1)=\tilde{y}L^{-1}(s)\omega_1-D_1|\tilde{y}|\leqslant \\ \qquad\qquad |\tilde{y}|\beta_1\sigma_{\rm M}-D_1|\tilde{y}|\leqslant 0, \\ \tilde{y}(\bar{\omega}_2+\bar{v}_2)=\tilde{y}L^{-1}(s)\omega_2 u-D_2|\tilde{y}|\leqslant \\ \qquad\qquad |\tilde{y}|\beta_2\sigma_{\rm M}u_{\rm d}-D_2|\tilde{y}|\leqslant 0. \end{cases} \tag{34}$$

Using the property of the trace of the matrix, one has

$$\begin{cases} {\rm tr}(\tilde{W}_1^{\rm T}\hat{\tilde{\sigma}}_1\tilde{y})=\tilde{y}\tilde{W}_1^{\rm T}\hat{\tilde{\sigma}}_1, \\ {\rm tr}(\tilde{W}_2^{\rm T}\hat{\tilde{\sigma}}_2\tilde{y}u)=\tilde{y}\tilde{W}_2^{\rm T}\hat{\tilde{\sigma}}_2 u. \end{cases} \tag{35}$$

Moreover, the following inequation always holds.

$$\tilde{z}^{\rm T}Q\tilde{z}\geqslant\lambda_{\min}(Q)\|\tilde{z}\|^2, \tag{36}$$

where $\lambda_{\min}(Q)$ is smallest eigenvalues of Q.

Submitting (34)−(36) into (32) yields

$$\begin{aligned} &\dot{V}= \\ &-\frac{1}{2}\tilde{z}^{\rm T}Q\tilde{z}+\tilde{y}\Delta-\tilde{y}\tilde{W}_1^{\rm T}\hat{\tilde{\sigma}}_1-\tilde{y}\tilde{W}_2^{\rm T}\hat{\tilde{\sigma}}_2 u+ \\ &{\rm tr}(\tilde{W}_1^{\rm T}\kappa_1|\tilde{y}|\hat{W}_1)+{\rm tr}(\tilde{W}_2^{\rm T}\kappa_2|\tilde{y}|\hat{W}_2)\leqslant \\ &|\tilde{y}|(\bar{\varepsilon}_1+\bar{\varepsilon}_2 u+\bar{d}_t+c_1\|\tilde{W}_1\|_{\rm F}+c_2\|\tilde{W}_2\|_{\rm F})- \\ &\frac{1}{2}\lambda_{\min}(Q)\|\tilde{z}\|^2+\kappa_1|\tilde{y}|{\rm tr}(\tilde{W}_1^{\rm T}(W_1-\tilde{W}_1))+ \\ &\kappa_2|\tilde{y}|{\rm tr}(\tilde{W}_2^{\rm T}(W_2-\tilde{W}_2)). \end{aligned} \tag{37}$$

According to (27), $\|\tilde{z}\|\geqslant\|y\|$, thus

$$-\lambda_{\min}(Q)\|\tilde{z}\|^2\leqslant-\lambda_{\min}(Q)|\tilde{y}|^2. \tag{38}$$

Since ${\rm tr}(\Theta_5^{\rm T}\Theta_5)=\|\Theta_5\|_{\rm F}^2$, the following inequation always holds.

$$\begin{cases} {\rm tr}(\tilde{W}_1^{\rm T}(W_1-\tilde{W}_1))\leqslant W_{1\rm M}\|\tilde{W}_1\|_{\rm F}-\|\tilde{W}_1\|_{\rm F}^2, \\ {\rm tr}(\tilde{W}_2^{\rm T}(W_2-\tilde{W}_2))\leqslant W_{2\rm M}\|\tilde{W}_2\|_{\rm F}-\|\tilde{W}_2\|_{\rm F}^2. \end{cases} \tag{39}$$

Submitting (38) and (39) into (37) yields

$$\begin{aligned} &\dot{V}\leqslant \\ &-\frac{1}{2}\lambda_{\min}(Q)|\tilde{y}|^2+|\tilde{y}|\sigma_{\rm M}(\varepsilon_1^*+\varepsilon_2^* u_{\rm d}+d_{\rm d})+ \\ &\kappa_1|\tilde{y}|(W_{1\rm M}\|\tilde{W}_1\|_{\rm F}-\|\tilde{W}_1\|_{\rm F}^2)+|\tilde{y}|c_1\|\tilde{W}_1\|_{\rm F}+ \\ &\kappa_2|\tilde{y}|(W_{2\rm M}\|\tilde{W}_2\|_{\rm F}-\|\tilde{W}_2\|_{\rm F}^2)+|\tilde{y}|c_2\|\tilde{W}_2\|_{\rm F}= \\ &-|\tilde{y}|[\frac{1}{2}\lambda_{\min}(Q)|\tilde{y}|-\sigma_{\rm M}(\varepsilon_1^*+\varepsilon_2^* u_{\rm d}+d_{\rm d})- \\ &\kappa_1(\alpha_1-\|\tilde{W}_1\|_{\rm F})\|\tilde{W}_1\|_{\rm F}- \\ &\kappa_2(\alpha_2-\|\tilde{W}_2\|_{\rm F})\|\tilde{W}_2\|_{\rm F}], \end{aligned} \tag{40}$$

where $\alpha_1=W_{1\rm M}+c_1/\kappa_1$ and $\alpha_2=W_{2\rm M}+c_2/\kappa_2$.

Moreover, we know that

$$\begin{cases} (\alpha_1-\|\tilde{W}_1\|_{\rm F})\|\tilde{W}_1\|_{\rm F}=\frac{1}{4}\alpha_1^2-(\|\tilde{W}_1\|_{\rm F}-\frac{1}{2}\alpha_1)^2, \\ (\alpha_2-\|\tilde{W}_2\|_{\rm F})\|\tilde{W}_2\|_{\rm F}=\frac{1}{4}\alpha_1^2-(\|\tilde{W}_2\|_{\rm F}-\frac{1}{2}\alpha_2)^2. \end{cases} \tag{41}$$

Submitting (41) into (40) leads to

$$\begin{aligned} \dot{V}\leqslant&-|\tilde{y}|[\frac{1}{2}\lambda_{\min}(Q)|\tilde{y}|-\sigma_{\rm M}(\varepsilon_1^*+\varepsilon_2^* u_{\rm d}+d_{\rm d})+ \\ &\kappa_1(\|\tilde{W}_1\|_{\rm F}-\frac{1}{2}\alpha_1)^2-\frac{1}{4}\kappa_1\alpha_1^2+ \\ &\kappa_2(\|\tilde{W}_2\|_{\rm F}-\frac{1}{2}\alpha_2)^2-\frac{1}{4}\kappa_2\alpha_2^2]. \end{aligned} \tag{42}$$

When $\lambda_{\min}(Q)<0$, the requirement for $\dot{V}\leqslant 0$ is

$$\begin{cases} \frac{1}{4}\lambda_{\min}(Q)|\tilde{y}|-\sigma_{\rm M}(\varepsilon_1^*+d_{\rm d})-\frac{1}{4}\kappa_1\alpha_1^2\geqslant 0, \\ \frac{1}{4}\lambda_{\min}(Q)|\tilde{y}|-\sigma_{\rm M}\varepsilon_2^* u_{\rm d}-\frac{1}{4}\kappa_2\alpha_2^2\geqslant 0. \end{cases} \tag{43}$$

That is

$$|\tilde{y}|\geqslant \max\{\frac{4\sigma_{\rm M}(\varepsilon_1^*+d_{\rm d})+\kappa_1\alpha_1^2}{\lambda_{\min}(Q)},\ \frac{4\sigma_{\rm M}\varepsilon_2^* u_{\rm d}+\kappa_2\alpha_2^2}{\lambda_{\min}(Q)}\}. \tag{44}$$

When $\lambda_{\min}(Q)>0$, the requirement for $\dot{V}\leqslant 0$ is

$$\begin{cases} \kappa_1(\|\tilde{W}_1\|_{\rm F}-\frac{1}{2}\alpha_1)^2-\sigma_{\rm M}(\varepsilon_1^*+d_{\rm d})-\frac{1}{4}\kappa_1\alpha_1^2\geqslant 0, \\ \kappa_2(\|\tilde{W}_2\|_{\rm F}-\frac{1}{2}\alpha_2)^2-\sigma_{\rm M}\varepsilon_2^* u_{\rm d}-\frac{1}{4}\kappa_2\alpha_2^2\geqslant 0. \end{cases} \tag{45}$$

That is

$$\begin{cases} \|\tilde{W}_1\|_{\rm F}\geqslant\frac{1}{2}\alpha_1+(\frac{\sigma_{\rm M}(\varepsilon_1^*+d_{\rm d})}{\kappa_1}+\frac{\alpha_1^2}{4})^{1/2}, \\ \|\tilde{W}_2\|_{\rm F}\geqslant\frac{1}{2}\alpha_2+(\frac{\sigma_{\rm M}\varepsilon_2^* u_{\rm d}}{\kappa_2}+\frac{\alpha_2^2}{4})^{1/2}. \end{cases} \tag{46}$$

Lemma 1[21] Given $x\in\mathbb{R}^n$ and a nonlinear function $h(x,t)$: $\mathbb{R}^n\to\mathbb{R}\times\mathbb{R}^n$, the differential equation

$$\dot{x}=h(x,t),\ t_0\leqslant t,\ x(t_0)=x_0, \tag{47}$$

has a differential solution $x(t)$ if $h(x,t)$ is continuous in $x(t)$ and t. The solution $x(t)$ is said to be uniformly ultimately bounded (UUB) if there exists a compact set $U\in\mathbb{R}^n$ such that, for all $x(t_0)=x_0\in U$, there exist a $\delta>0$ and a number $T(\delta,x_0)$ such that $x(t)<\delta$ for all $t\geqslant t_0+T$.

According to the above analyses and Lemma 1, $\|\tilde{z}\|$, $\|\tilde{W}_1\|_{\rm F}$ and $\|\tilde{W}_2\|_{\rm F}$ are UUB.

Next, we will show the boundedness of $\tilde{x}$. Let $\bar{\Delta}=\tilde{W}_1^{\rm T}\hat{\sigma}_1+\omega_1+\varepsilon_1^*+v_1+(\tilde{W}_2^{\rm T}\hat{\sigma}_2+\omega_2+\varepsilon_2^*)u+d_t+v_2$, (22) can be rewritten as

$$\dot{\tilde{x}}=(A-KC^{\rm T})\tilde{x}+b\bar{\Delta}. \tag{48}$$

The solution of $\dot{\tilde{x}}=(A-KC^{\rm T})\tilde{x}$ is

$$\tilde{x}(t)=\tilde{x}(0){\rm e}^{\int_0^t(A-KC^{\rm T}){\rm d}t}. \tag{49}$$

Further, the solution of (48) is

$$\begin{aligned} &\tilde{x}(t)= \\ &{\rm e}^{\int_0^t(A-KC^{\rm T}){\rm d}t}\int_0^t b\bar{\Delta}(\tau){\rm e}^{-\int_0^\tau(A-KC^{\rm T}){\rm d}\tau}{\rm d}\tau+ \\ &\tilde{x}(0){\rm e}^{\int_0^t(A-KC^{\rm T}){\rm d}t}= \\ &\Phi(t,0)\tilde{x}(0)+\int_0^t\Phi(t,\tau)b\bar{\Delta}(\tau){\rm d}\tau, \end{aligned} \tag{50}$$

where

$$\begin{cases} \Phi(t,0) = \mathrm{e}^{\int_0^t (A-KC^{\mathrm{T}})\mathrm{d}t}, \\ \Phi(t,\tau) = \mathrm{e}^{\int_0^t (A-KC^{\mathrm{T}})\mathrm{d}t - \int_0^\tau (A-KC^{\mathrm{T}})\mathrm{d}\tau}. \end{cases} \tag{51}$$

Since

$$\mathrm{e}^{\int_0^t (A-KC^{\mathrm{T}})\mathrm{d}t - \int_0^\tau (A-KC^{\mathrm{T}})\mathrm{d}\tau} = \mathrm{e}^{A(t-\tau)}\mathrm{e}^{-KC^{\mathrm{T}}(t-\tau)}, \tag{52}$$

the state transition matrix $\Phi(t,\tau)$ is bounded by $m_0\mathrm{e}^{-a(t-\tau)}$, where $m_0 = \mathrm{e}^{A(t-\tau)}$ and $a = KC^{\mathrm{T}}$ are positive constants.

Letting $\gamma = \omega_1 + \varepsilon_1^* + v_1 + (\omega_2 + \varepsilon_2^*)u + d_t + v_2$, then

$$\|\bar{\Delta}\|_2^a \leqslant \|\tilde{W}_1^{\mathrm{T}}\hat{\sigma}_1\|_2^a + \|\tilde{W}_2^{\mathrm{T}}\hat{\sigma}_2 u\|_2^a + \gamma_4, \tag{53}$$

where $\|\gamma\|_2^a \leqslant \gamma_4$.

Since $\|\Theta_6\|_2^a = \sqrt{\int_0^t \mathrm{e}^{-a(t-\tau)}\Theta_6^{\mathrm{T}}(\tau)\Theta_6(\tau)\mathrm{d}(\tau)}$ and $\|A\Theta_6\|_2 \leqslant \|A\|_{\mathrm{F}}\|\Theta_6\|_2$, one has

$$\begin{aligned} &\|\tilde{W}_1^{\mathrm{T}}\hat{\sigma}_1\|_2^a \leqslant \|\tilde{W}_1^{\mathrm{T}}\hat{\sigma}_1\|_{\mathrm{F}}^a\|\hat{\sigma}_1\|_2^a = \\ &\|\tilde{W}_1^{\mathrm{T}}\|_{\mathrm{F}}^a\|\hat{\sigma}_1\|\sqrt{\int_0^t \mathrm{e}^{-a(t-\tau)}\mathrm{d}(\tau)} = \\ &\|\tilde{W}_1^{\mathrm{T}}\|_{\mathrm{F}}^a\|\hat{\sigma}_1\|\sqrt{1-\mathrm{e}^{-at}}/\sqrt{a}. \end{aligned} \tag{54}$$

Similarly,

$$\|\tilde{W}_2^{\mathrm{T}}\hat{\sigma}_2 u\|_2^a \leqslant \|\tilde{W}_2^{\mathrm{T}}\|_{\mathrm{F}}^a\|\hat{\sigma}_2\|u_{\mathrm{d}}\sqrt{1-\mathrm{e}^{-at}}/\sqrt{a}. \tag{55}$$

Lemma 2[22] Consider the linear time-invariant system in state-space representation

$$\dot{x}(t) = Ax(t) + Bu(t),\ x(0) = x_0 \tag{56}$$

with $x(t) \in \mathbb{R}^n,\ u(t) \in \mathbb{R}^m,\ B \in \mathbb{R}^{n\times m}$. Then, every solution $x(t)$ of (56) satisfies

$$\|x(t)\| \leqslant k_1 + k_2\|u(t)\|_2^a, \tag{57}$$

where k_1 decays exponentially to zero, k_2 is a positive constant that depends on the eigenvalues of A.

Let $\gamma_5 = \|\hat{\sigma}_1\|(1-\mathrm{e}^{-at})$ and $\gamma_6 = \|\hat{\sigma}_2\|(1-\mathrm{e}^{-at})u_{\mathrm{d}}$. According to Lemma 2 and (53), we can get

$$\begin{aligned} \|\tilde{x}(t)\| \leqslant\ & k_1 + k_2\|\tilde{W}_1^{\mathrm{T}}\|_{\mathrm{F}}^a\gamma_5/\sqrt{a} + k_2\gamma_4 + \\ & k_2\|\tilde{W}_2^{\mathrm{T}}\|_{\mathrm{F}}^a\gamma_6/\sqrt{a} = \\ & \gamma_3' + \gamma_4'/\sqrt{a} + \gamma_5'\|\tilde{W}_1^{\mathrm{T}}\|_{\mathrm{F}}^a/\sqrt{a} + \\ & \gamma_6'\|\tilde{W}_2^{\mathrm{T}}\|_{\mathrm{F}}^a/\sqrt{a}, \end{aligned} \tag{58}$$

where $\gamma_3' = k_1,\ \gamma_4' = k_2\gamma_4\sqrt{a},\ \gamma_5' = k_2\gamma_5,\ \gamma_6' = k_2\gamma_6$; γ_3' decays exponentially to zero; $\gamma_4',\ \gamma_5'$ and γ_6' are positive constants.

Thus, $\|\tilde{x}(t)\|$ is bounded by $\|\tilde{W}_1^{\mathrm{T}}\|_{\mathrm{F}}$ and $\|\tilde{W}_2^{\mathrm{T}}\|_{\mathrm{F}}$, which have been verified to be bounded.

4 Controller design

In this section, we design the SMC based on the above approximators and the state observer to realize the trajectory tracking control of the DEA. In fact, there are other control methods that can be regarded as the candidates to achieve this control objective (such as, PID control method, fuzzy control method, backstepping control method and so on). However, the sliding mode control method itself has strong robust performance, and can effectively overcome the influence of the parameter uncertainty and the external disturbance on the system control[23]. Since the external disturbance is considered in the model of the DEA, we may as well design the SMC directly.

The sliding mode surface is chosen to be

$$S = c_{\mathrm{s}}e + \dot{e}, \tag{59}$$

where $e = \hat{x}_1 - \lambda_{\mathrm{d}},\ \dot{e} = \dot{\hat{x}}_2 - \dot{\lambda}_{\mathrm{d}};\ \lambda_{\mathrm{d}}$ and $\dot{\lambda}_{\mathrm{d}}$ are target values of the stretch of the DEA and the target rate of the stretch.

The Lyapunov function is constructed as

$$V_1 = \frac{1}{2}S^2. \tag{60}$$

According to (16), the derivative of V_1 is

$$\begin{aligned} \dot{V}_1 = S[&c_{\mathrm{s}}(\hat{x}_2 + K_1(x_1 - \hat{x}_1) - \dot{\lambda}_{\mathrm{d}}) + \hat{f}(\hat{x}) + \\ &\hat{g}(\hat{x})u + d_t - v + K_2(x_1 - \hat{x}_1) - \ddot{\lambda}_{\mathrm{d}}]. \end{aligned} \tag{61}$$

The controller is designed to be

$$\begin{aligned} u = & \\ &\frac{1}{\hat{g}(\hat{x})}[-c_{\mathrm{s}}(\hat{x}_2 + K_1(x_1 - \hat{x}_1) - \dot{\lambda}_{\mathrm{d}}) - \hat{f}(\hat{x}) + \\ &v - K_2(x_1 - \hat{x}_1) + \ddot{\lambda}_{\mathrm{d}} - \eta\mathrm{sgn}\,s], \end{aligned} \tag{62}$$

where $\ddot{\lambda}_{\mathrm{d}}$ is the target accelerated velocity of the stretch, $\eta \geqslant d_{\mathrm{d}} > 0$. $\hat{f}(\hat{x})$ and $\hat{g}(\hat{x})$ are given in (17).

Submitting (62) into (61) yields

$$\dot{V}_1 = d_t S - \eta|S| \leqslant 0. \tag{63}$$

When $\dot{V}_1 \equiv 0,\ S \equiv 0$. So, according to LaSalle's invariance theorem, we know that $e \to 0$ and $\dot{e} \to 0$ as $t \to \infty$. Since the convergence and boundedness of $\tilde{x}$ have been verified in the previous section, the trajectory tracking control of the DEA can be achieved by employing the above SMC (62) with the approximators (17) and the state observer (16). The structural diagram of the closed-loop control system is shown in Fig. 2.

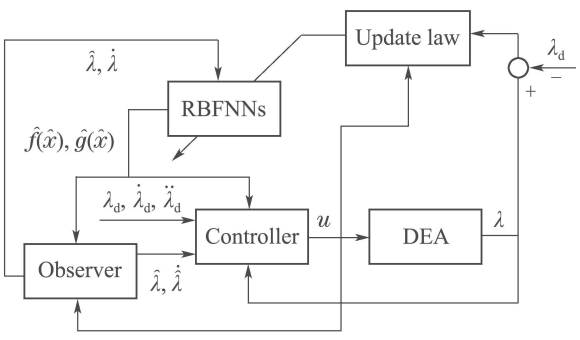

Fig. 2 Structural diagram of closed-loop control system

5 Simulations

In order to verify the effectiveness of the proposed control strategy, a simulation is carried out by using MATLAB tool. The model parameters of the DEA are shown in Table 1[24].

Table 1 Model parameters of DEA

Parameter	Value	Parameter	Value
L	0.02 m	$J_{\rm m}$	70
L_3	0.001 m	$\mu(T)$	0.097 MPa
ρ	960 kg/m^3	c	1.2

According to experimental results in [25],

$$\varepsilon(\lambda,T)=\varepsilon_0\varepsilon_{\rm r}(\lambda,T)=\varepsilon_0(\varepsilon_\infty+\frac{\rho}{T})[1+a_{\rm w}(2\lambda^{-\frac{1}{2}}-2)+b_{\rm w}(2\lambda^{-\frac{1}{2}}-2)^2+c_{\rm w}(2\lambda^{-\frac{1}{2}}-2)^3], \tag{64}$$

where $\varepsilon_0=8.85\times10^{-12}$(F/m) is the permittivity of vacuum;

$$\varepsilon_\infty=2.1,\ T=300,\ a_{\rm w}=-0.1658,\ b_{\rm w}=0.04086,\ c_{\rm w}=-0.003027;$$

and

$$\varepsilon(\lambda,T)=\varepsilon_0\varepsilon_{\rm r}(\lambda,T)=\varepsilon_0(\varepsilon_\infty+\frac{\rho}{T})[1+a_{\rm w}(2\lambda^{-\frac{1}{2}}-2)+b_{\rm w}(2\lambda^{-\frac{1}{2}}-2)^2+c_{\rm w}(2\lambda^{-\frac{1}{2}}-2)^3]. \tag{65}$$

The initial states of the DEA are chosen to be

$$\lambda_0=1.5,\ \dot\lambda_0=0. \tag{66}$$

So, the tensile forces are

$$P=\frac{\mu LL_3(\lambda_0-\lambda_0^{-5})}{1-\dfrac{2\lambda_0^2+\lambda_0^{-4}-3}{J_{\rm m}}}=2.7205. \tag{67}$$

The target trajectory is

$$\begin{cases}\lambda_{\rm d}=-0.5\cos t+2,\\ \dot\lambda_{\rm d}=0.5\sin t,\\ \ddot\lambda_{\rm d}=0.5\cos t.\end{cases} \tag{68}$$

The external disturbance is

$$d_t=10\sin(2t). \tag{69}$$

The parameters of two RBFNNs are:

$$N_1=N_2=7,$$
$$\chi'_{ij}=\chi''_{ij}=-4+j,\ i=1,2 \text{ and } j=1,2,\cdots,7,$$
$$\psi_i=6(i=1,2),$$

the initial values of the weights are $W_{ij}^0=0.1(i=1,2$ and $j=1,2,\cdots,7)$. The parameters of the observer are $k_1=4\times10^5$, $k_2=8\times10^7$. So, $H(s)=1/(s^2+4s+2200)$. Since

$$\mathrm{Re}[H(\mathrm{j}w)]=(8\times10^7-w^2)/((w^2-8\times10^7)^2+w^2 16\times10^{10})$$

may less than 0, $H(s)$ is not SPR. We choose $L^{-1}(s)=1/(s+3\times10^5)$ to ensure that $H(s)L(s)$ is SPR. The parameters of the controller (62) are

$$c_{\rm s}=7\times10^9,\ \eta=15.$$

In (31),

$$\kappa_1=0.1,\ \kappa_2=0.001,\ F_1=500,\ F_2=0.05.$$

In (33), $D_1=D_2=1.2$.

The simulation results are shown in Figs. 3–6. According to Figs. 3(a) and 3(b), λ and $\dot\lambda$ track $\lambda_{\rm d}$ and $\dot\lambda_{\rm d}$, respectively. The tracking error curves are shown in Fig. 4. Meanwhile, according to Figs. 3(c) and 3(d), the maximum observation error is about 1.76%. So, the designed approximators, state observer and SMC are effective. Moreover, according to Figs. 5(a) and 5(b), $\hat f(\hat x)$ and $\hat g(\hat x)$ do not converge to $f(x)$ and $g(x)$, respectively. It is because the input signal does not satisfy persistent excitation condition[26].

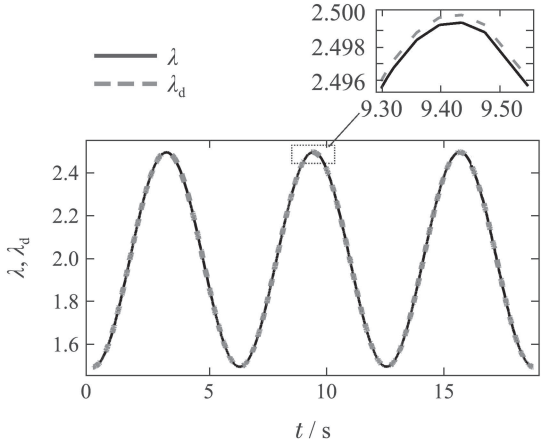

(a) Deformation tracking

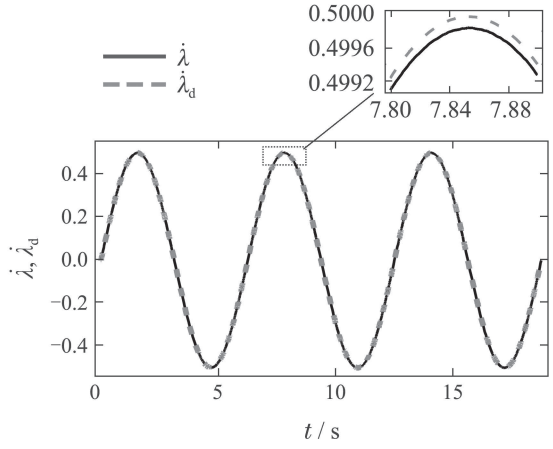

(b) Velocity tracking

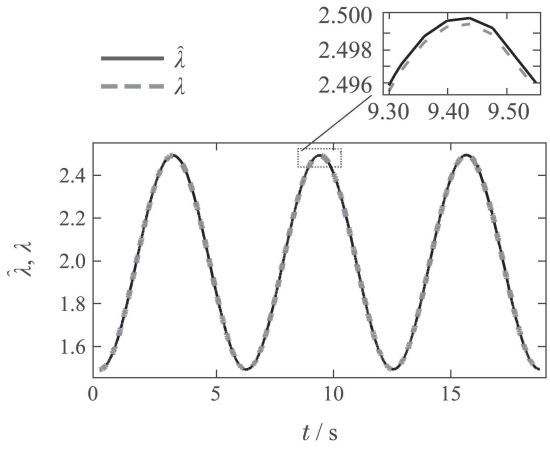

(c) Deformation observation

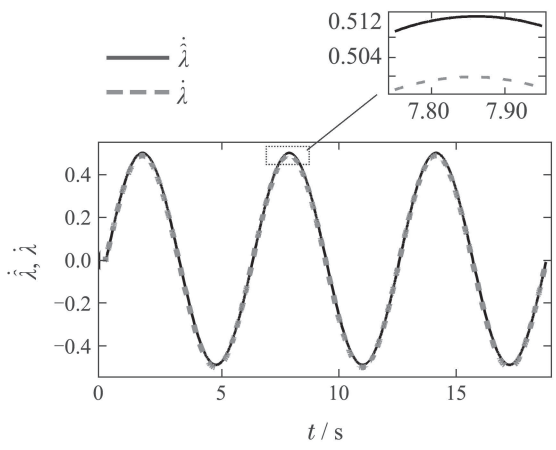

(d) Velocity observation

Fig. 3 Tracking results and observed results

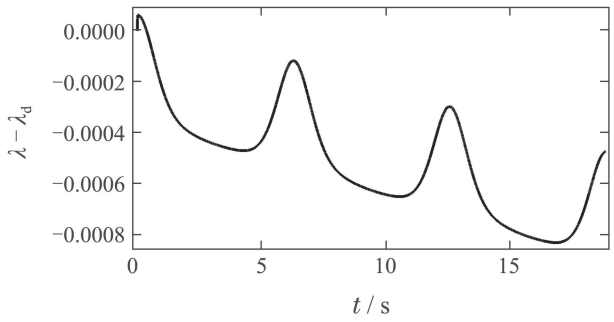

(a) Deformation tracking error

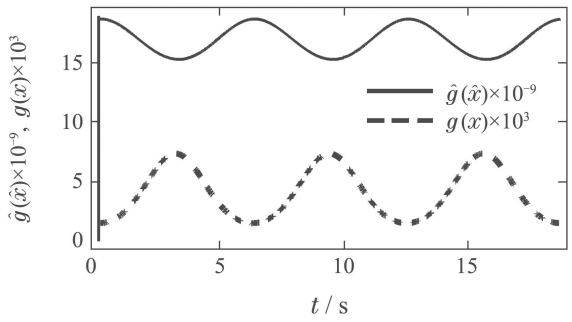

(b) Approximation results of $g(x)$

Fig. 5 Approximation results

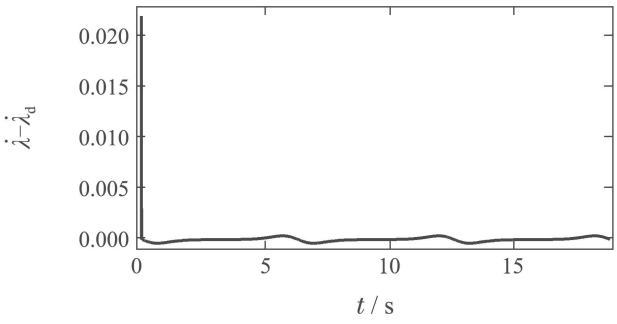

(b) Velocity tracking error

Fig. 4 Tracking error

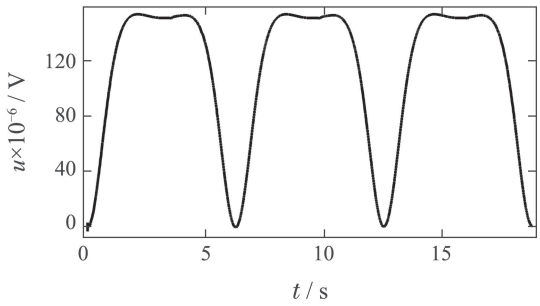

Fig. 6 Control input

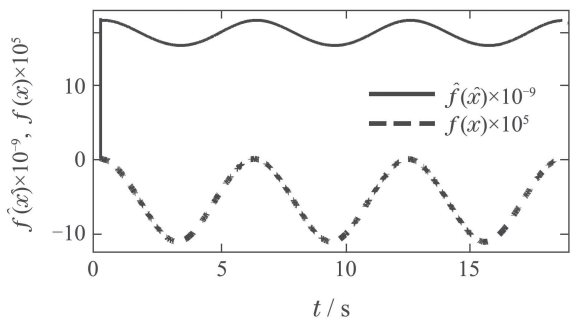

(a) Approximation results of $f(x)$

6 Conclusions

This paper proposes an adaptive robust control strategy for the DEA. Based on the RBFNNs, two approximators are used to estimate the unknown items of the DEA's model. Meantime, the state observer is designed to estimate the system states. Based on the approximation results and the observed states, the SMC is designed to realize the tracking control of the DEA.

The proposed control strategy only requires the stretch of the DEA, but does not require the the model parameters and the rate of the stretch. Thus, the proposed control strategy has adaptivity and robustness.

Moreover, the dynamic model (9) does not consider the creep and the hysteresis characteristics of the DEA. In the future, we will develop a more complex and more realistic mathematical model of the DEA to take the creep and the hysteresis into consideration. Furthermore, the control strategy proposed in this paper should be appropriately extended to meet the new model.

References:

[1] KOFOD G, KOENBLUH R. *Dielectric Elastomer Actuators as Intelligent Materials for Actuation, Sensing and Generation.* London: The Royal Society of Chemistry, 2008, chapter 16: 396 – 423.

[2] GU G Y, ZHU J, ZHU L M, et al. A survey on dielectric elastomer actuators for soft robots. *Bioinspiration and Biomimetics*, 2017, 12(1): 011003.

[3] BROCHU P, PEI Q B. Advances in dielectric elastomers for actuators and artificial muscles. *Macromoleculecular Rapid Communications*, 2010, 31(1): 10 – 36.

[4] O'HALLORAN A, O'MALLEY F, MCHUGH P. A review on dielectric elastomer actuators, technology, applications and challenges. *Journal of Applied Physics*, 2008, 104(7): 071101.

[5] MIRFAKHRAI T, MADDEN J D W, BAUGHMAN R H. Polymer artificial muscles. *Materials Today*, 2007, 10(4): 30 – 38.

[6] SHANKAR R, GHOSH T K, SPONTAK R J. Dielectric elastomers as next-generation polymeric actuators. *Soft Matter*, 2007, 3(9): 1116 – 1129.

[7] ROSSET S, NIKLAUS M, DUBOIS P, et al. Large-stroke dielectric elastomer actuators with ion-implanted electrodes. *Journal of Microelectromechanical Systems*, 2009, 18(6): 1300 – 1308.

[8] SOU Z G. Theory of dielectric elastomers. *Acta Mechanica Solida Sinica*, 2010, 23(6): 549 – 578.

[9] SARBAN R, LASSEN B, WILLATZEN M. Dynamic electromechanical modeling of dielectric elastomer actuators with metallic electrodes. *IEEE/ASME Transactions on Mechatronics*, 2012, 17(5): 960 – 967.

[10] GU G Y, GUPTA U, ZHU J, et al. Feedforward deformation control of a dielectric elastomer actuator based on a nonlinear dynamic model. *Applied Physics Letters*, 2015, 107(4): 042907.

[11] ROSSET S, O'BRIEN B M, Gisby T, et al. Self-sensing dielectric elastomer actuators in closed-loop operation. *Smart Materials and Structures*, 2013, 22(10): 104018.

[12] PELRINE R, KORNBLUH R, PEI Q, et al. High-speed electrically actuated elastomers with strain greater than 100%. *Science*, 2000, 287(5454): 836 – 839.

[13] LI T F, QU S X, YANG W. Electromechanical and dynamic analyses of tunable dielectric elastomer resonator. *International Journal of Solids and Structures*, 2012, 49(26): 3754 – 3761.

[14] XU B X, MUELLER R, THEIS A, et al. Dynamic analysis of dielectric elastomer actuators. *Applied Physics Letters*, 2012, 100(11): 112903.

[15] GENT A N. A new constitutive relation for rubber. *Rubber Chemistry and Technology*, 1996, 69(1): 59 – 61.

[16] PARK J, SANDBERG I W. Universal approximation using radial-basis-function networks. *Neural Computation*, 1991, 3(2): 246 – 257.

[17] CHEN T, CHEN H. Approximation capability to functions of several variables, nonlinear functionals, and operators by radial basis function neural networks. *IEEE Transactions on Neural Networks*, 1995, 6(4): 904 – 910.

[18] LV Y F, NA J, REN X M. Online H_∞ control for completely unknown nonlinear systems via an identifier-critic based ADP structure. *International Journal of Control*, 2017, DOI: 10.1080/00207179.2017.1381763.

[19] ZHAO J, WANG X, GAO G B, et al. Online adaptive parameter estimation for quadrotors. *Algorithms*, 2018, 11(11): 167.

[20] LABIOD S, BOUCHERIT M S, GUERRA T M. Adaptive fuzzy control of a class of MIMO nonlinear systems. *Fuzzy Sets and Systems*, 2005, 151(1): 59 – 77.

[21] LEWIS F L, DAWSON D M, ABDALLAH C T. *Control of Robot Manipulators*. London: Macmillan, 1993.

[22] IOANNOU P A, SUN J. *Robust Adaptive Control*. New Jersey: Prentice Hall, 1996.

[23] BARTOLINI G, PISANO A, PUNTA E, et al. A survey of applications of second-order sliding mode control to mechanical systems. *International Journal of Control*, 2003, 76(9/10): 875 – 892.

[24] KOFOD G. *Dielectric Elastomer Actuators*. Copenhagen: The Technical University of Denmark, 2001.

[25] SHENG J J, CHEN H L, LUI L, et al. Dynamic electromechanical performance of viscoelastic dielectric elastomers. *Journal of Applied Physics*, 2013, 114(13): 134101.

[26] SLOTINE J J E, LI W. *Applied Nonlinear Control*. New Jersey: Prentice Hall, 1991.

作者简介:

王亚午 副教授, 硕士生导师, 目前研究方向为软体机器人建模与控制, E-mail: wangyawu@cug.edu.cn;

叶雯珺 博士研究生, 目前研究方向为软体机器人建模与控制, E-mail: y_wenjun@encs.concordia.ca;

张一龙 副教授, 硕士生导师, 目前研究方向为软体机器人建模与控制, E-mail: zylnedu@yeah.net;

赖旭芝 教授, 博士生导师, 目前研究方向为非线性系统控制, E-mail: laixz@cug.edu.cn;

吴 敏 教授, 博士生导师, 目前研究方向为鲁棒控制与应用, E-mail: wumin@cug.edu.cn;

苏春翌 教授, 博士生导师, 目前研究方向为软体机器人建模与控制, E-mail: cysu@alcor.concordia.ca.